Available online at www.sciencedirect.com

SCIENCE DIRECT®

C. R. Physique 4 (2003) 105–113

COMPTES RENDUS PHYSIQUE

Optical telecommunications/Les télécommunications optiques

# Research trends in terrestrial transmission systems

# Orientations des recherches sur les systèmes de transmission terrestres

Sébastien Bigo *, Yann Frignac, Jean-Christophe Antona, Gabriel Charlet, Stéphanie Lanne

*Alcatel Research and Innovation, Route de Nozay, 91460 Marcoussis, France*

Received 18 October 2002

Presented by Guy Laval

**Abstract**

The technique of wavelength division multiplexing (WDM) has paved the way for multi-terabit/s capacities in terrestrial optical networks. Recently, we conducted a laboratory experiment to emulate a terrestrial transmission of 6.3 Tbit/s capacity over a record 2700 km distance. After describing some of the specific features of optical terrestrial transmission, we discuss the various technologies possibly involved in such an emulator and discuss their implementation in actual systems, namely the modulation format, the optical amplifier scheme, the 40 Gbit/s electronics and the forward error-correcting codes. ***To cite this article: S. Bigo et al., C. R. Physique 4 (2003).***



**Résumé**

La technique du multiplexage en longueur d'onde a permis l'émergence de débits multi-Terabit/s dans les réseaux optiques terrestres. Récemment, nous avons réalisé en laboratoire une transmission en environnement terrestre de données à 6.3 Tbit/s sur la distance record de 2700 km. Après avoir décrit les particularités des transmissions optiques terrestres, nous détaillons les différentes technologies qui peuvent être utilisées pour atteindre un tel objectif, à savoir le format de modulation, la configuration des amplificateurs optiques, l'électronique à 40 Gbit/s et les codes correcteurs d'erreurs. ***Pour citer cet article : S. Bigo et al., C. R. Physique 4 (2003).***



*Keywords:* Transmission; Optical fiber; Nonlinear optics; Erbium-doped fiber amplifiers; Raman amplifiers; Telecommunication networks

*Mots-clés :* Transmission ; Fibre optique ; Optique non-linéaire ; Amplificateur à fibre dopée erbium ; Amplificateur Raman ; Réseaux de télécommunication

## 1. Introduction

At the opening of the millennium, the capacity of terrestrial telecommunication systems has experienced a thousand-fold increase, which happened in just over ten years. This revolution is mostly the result of an optimal use of the optical amplifier bandwidth, through the technique of Wavelength-Division Multiplexing (WDM) [1]. The benefits of WDM have been widely

* Corresponding author.
*E-mail address:* Sebastien.Bigo@alcatel.fr (S. Bigo).

1631-0705/03/$ – see front matter © 2003 Académie des sciences/Éditions scientifiques et médicales Elsevier SAS. Tous droits réservés.
doi:10.1016/S1631-0705(02)00007-5

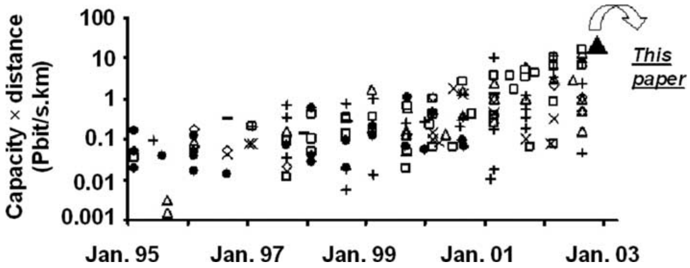


Fig. 1. Capacity × distance product of WDM terrestrial laboratory experiments reported since 1995.

demonstrated over the multiple laboratory experiments reported over the past years (see [2–17] for the most significant since mid 2001). It has been customary to rank these experiments as a function of the capacity × distance ($C \times D$) parameter, to reflect both the difficulty of generating high capacity multiplexes and of transmitting them over long distances.

Fig. 1 depicts the evolution of the $C \times D$ of the major research system experiments reported to date, since 1995. The $C \times D$ is found to follow a continuous exponential growth, surprisingly insensitive to the fluctuations of the economic environment, at least up to now. This evolution corresponds to an approximate quadrupling of the $C \times D$ every 10 years. Most remarkably, if we extended Fig. 1's data to the early days of the optical communications industry [18], i.e., in the early 1970s, we would find that the growth rate has been virtually the same for 30 years. Thus, the term of 'revolution', often heard to qualify the WDM era, is not really appropriate. More accurately, it seems that there is an empirical law predicting a growth rate for the whole field of photonics (×2 every 16 months), which is higher than the famous Moore's law for electronics (×2 every 18 months) [1].

In Fig. 1, we show the data point corresponding to our most recent transmission of 6.3 Tbit/s data over 2700 km. To our knowledge, this result represents the largest $C \times D$ demonstrated to date in terrestrial systems at 17 Pbit/s·km. It is also an improvement from our previous result of [2]. Clearly, this is a WDM-based experiment, but it combines a number of other very promising technologies, which are not yet implemented in actual systems. Along with a detailed description of this experiment, we shall provide here overview of the research trends in terrestrial optical networks, with emphasis on modulation formats, optical amplifier configurations, transmission fiber types, 40 Gbit/s electronics and forward error-correcting (FEC) codes.

## 2. Characteristics of terrestrial systems

Our 6.3 Tbit/s experiment described here emulates a realistic point-to-point system with periodic amplification. The system includes concatenated sections of single-mode fiber separated by optical repeaters, linking a transmitter and a receiver. In terrestrial networks, such systems conventionally carry information over distances of a few 100 kilometers to 1000 kilometers, typically, as referred to as long-haul (LH) distances. In recent years, operators have requested ultra-long haul (ULH) distances (i.e., over 1000 km), making terrestrial networks sizes grow closer to that of submarine networks. However, the two networks types differ from several features other than mere transmission distance. Submarine systems are mainly designed on a prototyped, customized basis. Terrestrial systems must be flexible in order to be adaptable to complex existing networks topologies, as dictated by geography, legacy (development history) and land/real-estate issues. In such topologies, the repeater spacing varies along the signal path, and is usually much longer than in submarine links. Laboratory experiments must comply with this requirement, though the repeater spacing is generally made constant for simplicity. Fig. 2 recapitulates different spacing configurations as well as the total link length used in most significant WDM laboratory experiments reported to date (including that of Fig. 1), whether complying with submarine or LH/ULH terrestrial configurations. The last two can easily be separated from the first, owing to their smaller amplifier spacings, typically ranging within [80–120 km], as opposed to [30–50 km]. Besides these three classes of WDM transmission experiments, Fig. 2 shows a fourth, corresponding to a smaller market segment, namely that of submarine repeater-less transmission. This class refers to systems where the distance between the transmitter and the receiver can exceed a few hundreds of kilometers without in-line regenerating stage, which can only be obtained with specific technologies.

In terrestrial systems, the average fiber transmission loss is also generally higher than in submarine links, owing to numerous splices during cable installation and cut repairs. Therefore, a higher optical power must be launched into the transmission fiber, which keeps the signal-to-noise ratio (SNR) within receiver requirements. However, the higher the power, the more the optical data waveforms are altered when propagating in the fiber, as a result of nonlinear (essentially Kerr-like) effects. Paradoxically, terrestrial links can suffer from similar nonlinearity impairments, if not more than submarine links, regardless of the difference in transmission distances. The greatest difference between terrestrial and submarine networks could be that in the second case, designers can choose an 'ideal' fiber scheme, whereas in the first case operators generally demand one to re-use their existing

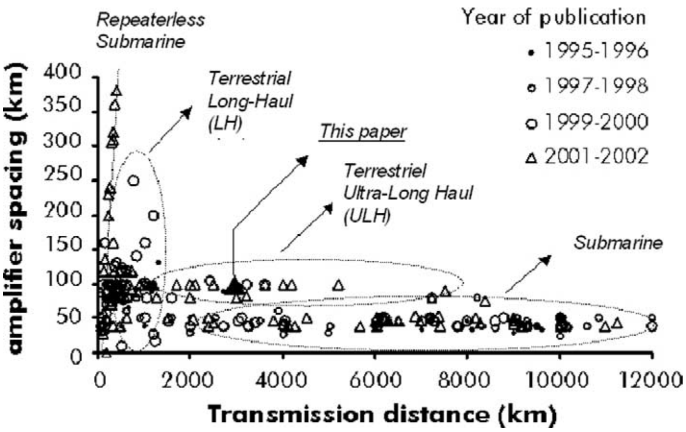


Fig. 2. Fours segments of the optical transmission market classified by (distance, amplifier spacing) pairs. The dots correspond to laboratory experiments reported at major telecommunications conferences.

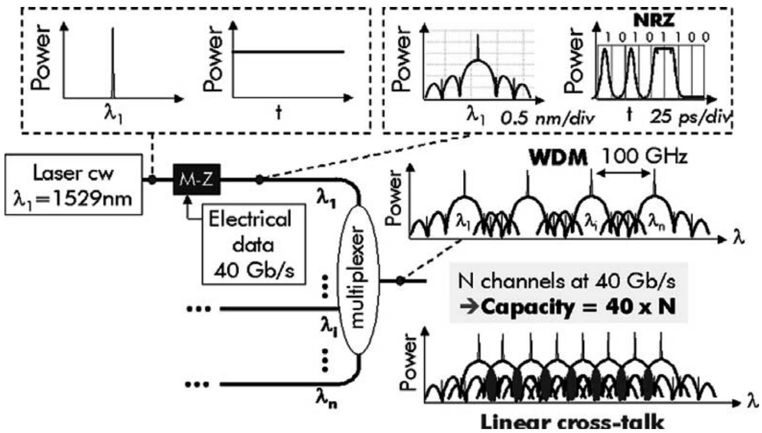


Fig. 3. Linear cross-talk in high capacity WDM systems.

fiber cable-plant, regardless of its inherited imperfections. The cost of deploying new terrestrial cable infrastructure can be forbidding. Civil engineering alone can represent indeed up to 85% of the total system cost. For terrestrial operators, capacity increases are primarily obtained by upgrading terminal equipments and repeaters. This specific cost-related issue has largely caused the popularity of WDM technologies, especially when in the early days of WDM, where fiber shortage came out as a major concern.

## 3. Capacity limitations at high information spectral densities

WDM is based on combining together into the same fiber $n$ optical channels, generated out of $n$ laser diodes at $n$ different carrier wavelengths, as depicted in Fig. 3. All these laser diodes are modulated, which means that they carry digital information coming from electrical streams of bits. The most straightforward way to modulate a laser diode at $B$ Gbit/s (e.g., 40 Gbit/s) is to switch its output light ON or OFF, whether the symbol to be transmitted is a mark (‘1’) or a space (‘0’), at a rate equal to the information frequency B GHz (e.g., 40 GHz). This operation produces so-called *Non-Return-to-Zero* (NRZ) data, as schematized in the inset in Fig. 3. Switching is often performed by an external electro-optic modulator in a Mach–Zenhder (M–Z) interferometric configuration. Provided that this operation only affects the intensity of light and not its phase, basic Fourier theory predicts that NRZ modulation turns the monochromatic spectrum of a laser diode into an optical spectrum of finite bandwidth. Such NRZ spectrum involves a carrier and two side-lobes and occupies approximately twice the information frequency (see inset in Fig. 3).

In an actual WDM system, each channel $i$ at wavelength $\lambda_i$ is modulated with its specific data stream and combined with the other channels through a passive multiplexer based on optical filter-like technologies. At the receiver side, a demultiplexer based on the same kind of technologies is used to filter channel $i$ out of its neighbors. In the beginnings of the WDM era, these multi/demultiplexing filtering technologies could be viewed up as stumbling blocks to the denser implementation of channels and thus the enhancement of system capacity, simply because the bandwidths of optical filters were not narrow enough to reject close neighboring channels. Now that these technologies have improved, WDM system designers are left with more fundamental limitations coming from the channel bandwidths themselves, as illustrated in Fig. 3. Because the bandwidth of channels is finite, the spectra of neighboring channels unavoidably overlap when the channel spacing $\Delta f$ is reduced, producing detrimental linear cross-talk.

A conventional indicator of this overlap is the bandwidth utilization ratio, also referred to as the information spectral density $\theta$. It is derived from the information frequency $B$ with $\theta = B/\Delta f$. Linear cross-talk sets a limit to the ultimate capacity that can be transmitted within a given bandwidth. Assuming conventional intensity-modulated signals like NRZ signals, 1 bit/s/Hz spectral density seems to stand as a maximum, but the radio communication field has taught us that specific coding techniques should still let us multiply this figure by a few units. However, with state-of-the art spectral densities at 0.2 bit/s/Hz in commercial NRZ systems (i.e., 50 GHz-spaced channels at 10 Gbit/s covering the entire amplifier bandwidth), and an already high 0.4 bit/s/Hz foreseen in the next generation of WDM products (i.e., 25 GHz-spaced channels at 10 Gbit/s), it can be easily figured out that increasing the channel rate by four will not automatically bring capacities greater by the same amount. As an example, while current high capacity commercial systems use 10 GHz electronics, a growing number of research experiments, including the one detailed in this paper, have been resorting to the 40 Gbit/s channel rate. Assuming NRZ format, the overlap between neighboring WDM channels is as stringent with 100 GHz spaced channels at 40 Gbit/s (see Fig. 3), as with 25 GHz-spaced channels at 10 Gbit/s, while the maximum total capacity is just the same. Thus, moving from 10 Gbit/s to 40 Gbit/s channel rate is only interesting in terms of capacity if the spectral density is increased at the same time. To that purpose, modulation formats alternative to NRZ have been receiving a considerable attention in the past few years.

## 4. Modulation formats

These alternative formats rely on intensity modulation (IM), phase modulation (PM), or any linear combination thereof. Regardless of complexity and cost considerations in the implementation, the pros and cons of formats should not be limited to the sole issue of compatibility with high information spectral densities. Some of them can be immediately recommended for their superior robustness to fiber nonlinearity, others because they exhibit greater tolerance to amplifier noise accumulation. Others have higher resistance to the linear dependence of the fiber index of refraction, namely to the chromatic dispersion, or to random fluctuations of the birefringence along the fiber, namely to the Polarization Mode dispersion (PMD). Not surprisingly, one is not able to simultaneously combine all these advantages in a single format.

The *return-to-zero format* (RZ) is often viewed as a promising alternative to NRZ. With RZ, any ‘1’ symbol is represented by a pulse, which can be of variable duration. RZ is known for higher tolerance to fiber nonlinearity. An intuitive explanation for this feature is the fact that with isolated pulses, unlike in NRZ sequences, each ‘1’ symbol (1) is virtually independent from its neighbors, and (2) experiences the same nonlinearity. In NRZ, sequences of ‘1’ emulate cw light-signals packets, which are unstable under nonlinear propagation at the edges. Solitons do not represent a format but a particular transmission regime for RZ signals, where chromatic dispersion and fiber nonlinearity cancel each other, provided that a specific pulse power is launched into the line. Various promising demonstrations were carried out in the laboratories [19]. However, over terrestrial distances, solitons were never been shown to outperform traditional NRZ systems. The main limitation of soliton propagation is nonlinear crosstalk, which can be very penalizing with only a few numbers of WDM channels. Besides their resistance to nonlinear impairments, RZ data have the additional advantage of being inherently more tolerant to PMD than NRZ.

Several enhanced RZ formats have been proposed as alternatives to conventional RZ. They differ from each other by a non-uniform specific phase. The carrier-suppressed RZ (CS-RZ) format was initially used in terrestrial links at 40 Gbit/s channel rate [20]. Two neighboring CS-RZ pulses have the particularity of having phases that differ by $\pi$. The phase profile of CS-RZ format helps limit inter-symbol interference and improve the tolerance to nonlinear effects with respect to RZ. Though only applied in submarine demonstrations, Chirped RZ (C-RZ) format performs even better in this matter [21]. Its superior resistance to nonlinearities has nonetheless been obtained at the expense of a larger channel spectral occupancy, which limits the maximum achievable spectral efficiency. This issue was addressed [22] and alternate-chirped RZ (AC-RZ) format which has most of the advantages of the C-RZ format, but a reduced channel bandwidth.

Another class of formats devoted to spectrally dense WDM systems involve truncating the channel optical spectra using very narrow, and thus bandwidth-limiting (BL), optical filters. This class includes *single-side band* (SSB) or *vestigial side-band* (VSB) modulation. The basic principle is to eliminate the redundancy of information in the two side-bands forming an NRZ or RZ spectrum spectrum. Only one side-band is then transmitted while leaving a fraction of the carrier (VSB technique) or completely suppressing the carrier (SSB technique). VSB obtained by narrow, off-center optical filtering has proved efficient to support densely-packed WDM channels [23], but the maximum achievable distance is limited by the fact that the suppressed part of the channel spectrum tends to reconstruct itself through nonlinearities. This suggests using VSB filtering only at receiver side, but with a specific, nonequidistant, frequency allocation scheme. Using this scheme, a laboratory experiment was conducted to demonstrate the transmission of 128 NRZ-VSB channels at 40 Gbit/s bit-rate, totalizing 5 Tbit/s capacity, over a distance of 1500 km [13]. The spectral density was 0.64 bit/s/Hz, involving WDM channels spaced by an average 62.5 GHz. By using VSB NRZ filtering both at the transmitter and the receiver sides, a higher spectral density was achieved at 0.8 bit/s/Hz, with 40 Gbit/s channels spaced by just 50 GHz, but the transmission distance of the WDM channels was limited to 900 km [8]. This distance was later improved to 1280 km, also by truncating the spectrum of each channel by narrow filtering, but based another format, namely Carrier-Suppressed Return-to-Zero (CS-RZ) [4].

In the experiment described here, the same 0.8 bit/s/Hz spectral density is used to transmit data at 6.3 Tbit/s over 2700 km, while relying on a modulation format based on *duo-binary modulation*. Duo-binary is a three-level coding scheme, involving '0' symbols, as well as '+1' and '−1' symbols, which differ by optical $\pi$-phase shifts. It is especially interesting for dense WDM applications, since it has been optimized to reduce the channel bandwidth. From a practical standpoint, the conventional method to convert an incoming electrical binary data into an optical duobinary signal is to feed a dual-drive Mach–Zehnder (M–Z) modulator with two complementary sets of the data, after passing them into low pass (here, 12 GHz cutoff frequency) Bessel electrical filters as schematized in Fig. 4 (line 2). This process scrambles the incoming binary stream. Therefore, differential electrical precoders would have to be inserted before the M–Z, in order to recover the initial data with a conventional NRZ receiver. However, in our laboratory experiment, such a precoder is not necessary, because our test binary sequences, referred to as pseudo-random bit-sequences (PRBS), have the remarkable property of being unchanged by the aforementioned generation process.

Fig. 4, line 2 depicts the example computed waveform of an eight-bit binary sequence with corresponding intensity, phase, and eye-diagram. The associated optical spectra, is also drawn and can be compared with that of NRZ data (Fig. 4, line 1), showing effective reduction of bandwidth and suppression of the carrier. While the intensity profile of a pure duobinary signal should ideally be very similar to that of NRZ, it can observed that the conventional generation process leaves a small fraction of light within '0' symbols, which incorporate $\pi$-phase shifts in their center. This feature was found to contain the spreading of the '$\pm 1$' symbols upon propagation in a dispersive optical fiber, yielding a threefold better tolerance to chromatic dispersion than NRZ or pure duobinary [16]. Owing to this specific property, the modulation format has been renamed *phase-shaped binary transmission*, or PSBT [24]. However, the drawback of PSBT is a poor eye-opening and thus a poor tolerance to noise (Fig. 4, line 2). This can be circumvented by passing the PSBT signal through a second M–Z with NRZ modulation [25] to yield Enhanced-PSBT (E-PSBT), as depicted in the third schematic of Fig. 4. This approach effectively reduces the residual light in the '0's, while leaving the beneficial $\pi$-phase shifts in their center. Surprisingly, the main lobe of the resulting E-PSBT computed optical spectrum appears narrowed with respect to that of PSBT. This suggests using one or several narrow, BL optical filter(s) to also get an improved noise tolerance, with a simpler, less expensive set-up. Besides, the compatibility with the densest implementations of WDM systems is enhanced. The computed eye-diagram and spectrum obtained after passing the PSBT data through such filters, located in the transmitter (3 dB bandwidth = 50 GHz) and in the receiver (3 dB bandwidth = 40 GHz) are also shown in Fig. 4 (line 3). The eye-opening of BL-PSBT is noticeably improved with respect to that of PSBT. After actual implementation with filters of similar characteristics to in the simulation, we measured 2.9 dB sensitivity reduction to noise at a bit-error rate of $10^{-5}$ with our BL-PSBT equipment, as compared to PSBT.

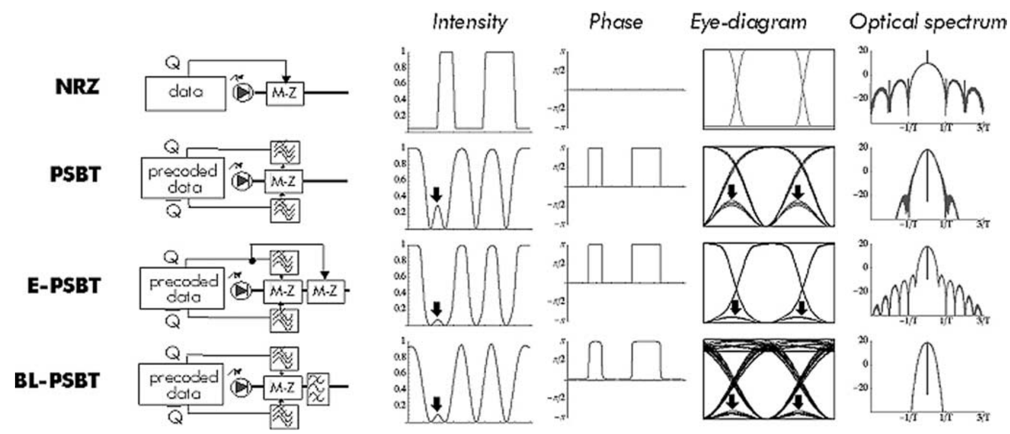


Fig. 4. Computed typical characteristics of Phase-Shaped Binary Transmission (PSBT), Enhanced PSBT (E-PSBT), and Bandwidth-Limited-PSBT (BL-PSBT) and layout of the generation process. The arrows on the intensity traces indicate the residual fraction of light within '0' symbols.

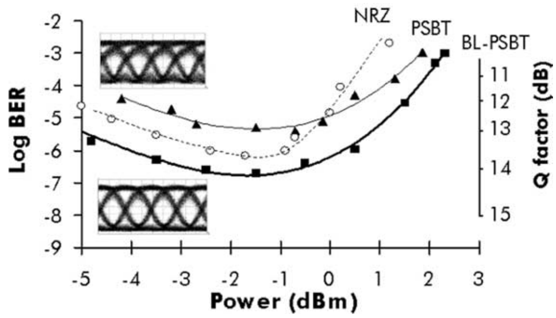


Fig. 5. Impact of single-channel nonlinear effects measured at 1200 km distance (inset = eye diagrams at 0 km).

Tolerance or robustness to nonlinear effects is another essential feature to investigate, in order to assess the compatibility of BL-PSBT format with long-distance transmission. This tolerance can be measured by varying the power at the beginning of each fiber span along the link. In Fig. 5, we have plotted the $Q$ factor [1], derived the corresponding bit-error-rates (BER $= f(Q)$), as measured at 1200 km distance, with NRZ, PSBT and BL-PSBT modulation formats, using a single 40 Gbit/s channel in link (see later for details). For consistent cross-comparisons, the link dispersion characteristics were optimized for each format. At relatively low power, when noise impairments dominate, the $Q$ factor of PSBT is penalized by 0.9 dB with respect to NRZ, whereas that of BL-PSBT is improved by 0.7 dB. This is the result of waveform reshaping caused by the narrow optical filters, illustrated by the eye-diagrams of Fig. 5 insets. NRZ is found to suffer from stronger nonlinear degradations than the PSBT formats when power is increased, e.g., at $Q$ factor = 10 dB, the BL-PSBT can tolerate a 1.5 dB higher power than NRZ [2]. Furthermore, in WDM operation, 50 GHz-spaced neighboring channels caused a $Q$-factor penalty no higher than 0.3 dB due to the linear/nonlinear crosstalk.

## 5. The amplifier scheme

In order to compensate for fiber loss, we need to periodically amplify the 6.3 Tbit/s multiplex. To comply with terrestrial constraints (Fig. 2), we decided to locate the optical repeaters every 100 km in our experiment. We use erbium-doped fiber amplifiers (EDFAs), assisted with distributed Raman amplification for that purpose.

It is the relatively large bandwidth of EDFAs that originally fostered the introduction of the WDM technique in optical systems. However, to be practical, the technique requires homogeneous propagation of all the channels throughout the overall link, which demands flat-gain EDFAs. In the early 1990s, fluoride-based EDFAs with inherent flat-gain characteristics had been proposed, but this technology was soon supplanted by regular silica-based EDFAs equipped with gain flattening filters (GFFs). The GFFs have a transfer function opposite to the natural gain excursion of the erbium gain. However, the larger the EDFA bandwidth, the more lossy the GFFs, and, hence, the poorer the noise characteristics of the amplifiers. Thus, to provide flat gain to our 158 channels, i.e., to a total $158 \times 50$ GHz = 7.9 THz bandwidth, we have to use two EDFAs operating in parallel, each of them providing flat gain over approximately a 4-THz bandwidth, namely over the so-called C-band [1530–1562 nm] and L-band [1569–1602 nm]. Those two EDFAs differ essentially by the lengths of the erbium-doped fibers and by their GFFs. At the input and the output of the repeaters, specific multiplexing filters need to be inserted to separate and combine the two bands. Note that, up to now, such dual-band repeaters have only been used in laboratory experiments, and have not yet been implemented in the field.

Beside the dual-band EDFAs, we use Raman amplification in the transmission fiber to minimize the noise brought by each repeater. The principle can be simply described as follows. At each repeater, before the EDFA(s), a strong continuous wave is launched (generally backwards) into the transmission fiber, as schematized in Fig. 6(a) (top). Through Stimulated Raman Scattering (SRS), this wave serves as a pump to amplify the WDM channels propagating in the opposite direction, provided that its wavelength is approximately 100 nm smaller than the spectral region where gain is needed. This scheme can improve the SNR because it is a distributed process, in contrast to the lumped scheme involved in EDFAs. A better insight into this phenomenon can be obtained by computing the relative change in signal power along a 100 km span, as drawn in Fig. 6(a). In the presence of 15 dB Raman amplification (full line), the power decay resulting from fiber loss is stopped at about 20 km before the next repeater. At this point, the power level is $\delta P = 6$ dB higher than at the input of a regular EDFA (dotted line). This minimum power level in the span $P_{\min}$ mainly sets the amount of noise generated by the overall amplification process. Therefore, deploying Raman amplifiers effectively reduces the span loss by several dB ($\sim \delta P$), or else effectively increases the SNR by the same amount. Naturally, SRS provides gain only over a limited wavelength region, and gain flatness is generally obtained by sending several pumps at different wavelengths simultaneously into the transmission fiber. In our

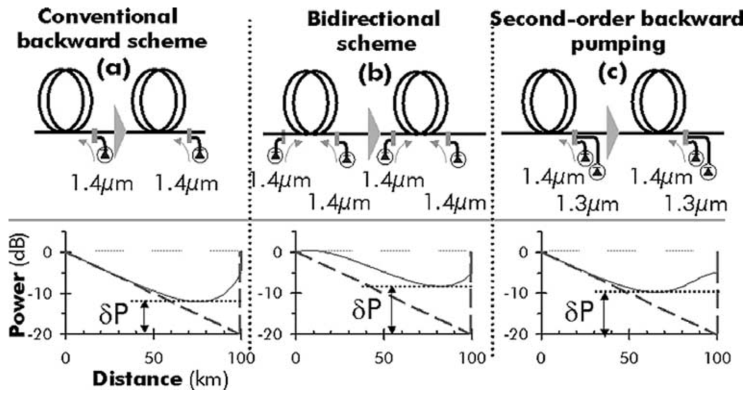


Fig. 6. Schematics of (a) Raman-assisted EDFAs with 1.4 µm pumping (top) in the conventional configuration; (b) improved by bi-directional pumping; (c) or second-order Raman pumping. Assuming 100 km-long fiber spans and 15 dB total Raman gain, the signal power evolution has been computed (full line) as compared to a lumped EDFA (dotted line).

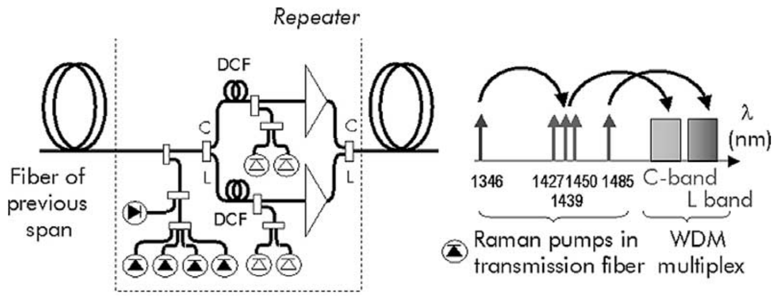


Fig. 7. Schematic of our experimental repeaters (left) involving three successive stages: Raman amplification in the transmission line according a specific wavelength allocation (right), followed by individual Raman amplifier in DCF and EDFA for each of two wavelength bands.

6.3 Tbit/s experiment, we use three pumps at 1427 nm, 1439 nm 1450 nm providing gain to the C band, and one pump at 1485 nm providing gain to the L band, all sent backwards in each fiber span.

Two approaches can be used to further improve the noise performance of such dual-band Raman-assisted EDFAs. The first one consists in sending the Raman pumps not only in the backward direction but also in the forward direction (Fig. 6(b)). The second one has been implemented in our experiment. It consists in sending along with all the other pumps, the light from a fibre laser at wavelength 1346 nm (Fig. 6(c)). This light act as a secondary pump for the other pumps (here, mostly at 1427 and 1439 nm) limiting their decay along the fiber. In both approaches, the minimal power level in the span $P_{\min}$ is increased (i.e., $\delta P$ is increased), as computed in Figs. 6(b) and 6(c). This reduces the noise generated by the overall repeater. We estimate at 1 dB the gain on the signal-to-noise ratio obtained using the second-order pumping technique. Naturally, the two approaches (b) and (c) are not contradictory and could be mixed together.

Besides, repeaters generally incorporate sections of dispersion compensating fibers (DCFs) located before the EDFA(s). These DCFs have dispersion characteristics opposite to that of the transmission fiber, such that any detrimental waveform distortions due to chromatic dispersion can be contained. However, a proper repeater design demands that the power decay within these fiber sections does not bring signal power below the minimum power level $P_{\min}$ defined above, which would strongly lower the benefits of Raman amplification in the transmission fiber. Thus, the loss of the DCF generally should be pre-compensated by some form of optical pre-amplification, again based on SRS in our experiment. To this end, four other pumps at 1423 nm and 1455 nm in C Band, and 1470 nm and 1500 nm in L band also provide Raman gain in the DCFs. The resulting repeater configuration is summarized in Fig. 7.

## 6. The loop experiment itself

The set-up of the 6.3 Tbit/s laboratory experiment is shown in Fig. 8. The WDM transmitter consists of 158 lasers diodes with wavelengths ranging from 1529.94 nm to 1561.42 nm in the C-band and 1569.59 nm to 1602.31 nm in the L-band. Because of obvious cost issues, all the lasers are not modulated with independent information, but in each band, are

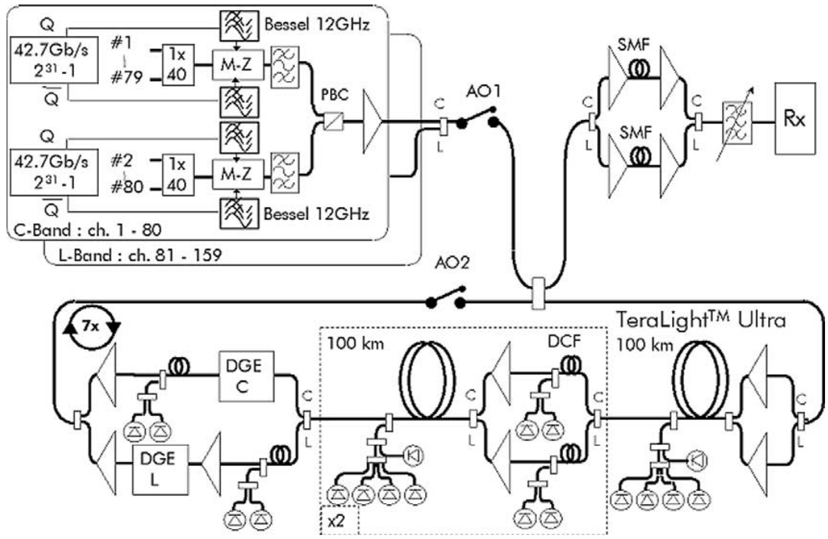


Fig. 8. Recirculating loop set-up.

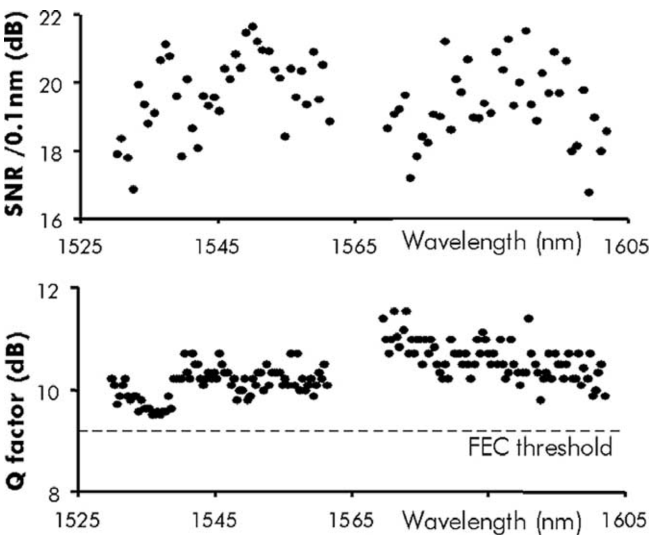


Fig. 9. Experimental results.

combined into two sets of 100 GHz-spaced channels, corresponding to odd and even channels respectively, through $1 \times 40$ array-waveguide multiplexers. These sets are modulated independently with PSBT format by $2^{31}$–1 bit-long pseudo-random bit sequences (PRBS). These PRBS are produced electrically out of four sequences at 10 Gbit/s with 7% overhead data, i.e., at 10.7 Gbit/s. The overhead emulates the presence of forward error correction (FEC), a very digital technique to correct errors in the received data stream [1], which is now part of all WDM transmission systems.

The resulting odd and even PSBT channels are passed into periodical narrow filters to form BL-PSBT channels before being interleaved with orthogonal polarisations through polarisation-beam combiners (PBC), boosted, passed into an acousto-optic switch (AO1) and sent into our 300 km long re-circulating loop, via the loop coupler.

A loop is a convenient way to emulate a transmission over very long distances, without resorting to the required amount of fiber and repeaters. It incorporates a switch AO2, which, like AO1, is controlled by delays generators, triggering the measuring equipment synchronously with the loop. Initially, the loop is filled with a flow of data by closing AO1, while opening AO2. Then, AO2 is closed and AO1 opened at time $t_0$, which initiates the circulation of the loaded data. A fraction of the light from these data is continuously extracted via the loop coupler and sent to the receiver photodiode. The transmission quality is evaluated by comparing the received data sequence with the initial one. The number of errors per second forms the bit-error rate

(BER). This BER is measured only within a small gating window starting at time $t > t_0$, to select only the data having traveled a given number $n$ of round trips (i.e., a given distance), $n$ being simply derived out the loop trip time and $t - t_0$.

The loop itself consists of three 100 km long spans of Alcatel TeraLight™ Ultra fiber, a fiber specifically designed for ultra-long haul applications [13]. This fiber has a chromatic dispersion of 8 ps/nm·km, dispersion slope of 0.052 ps/nm$^2$·km, loss of 0.20 dB/km and effective area of 63 µm$^2$ at 1.55 µm. The fiber spans are separated by the above described repeaters, providing a total 17.0 dBm and 15.5 dBm power in C and L-band, respectively. A dynamic gain equalizer (DGE) is inserted into the last repeater of the loop in order to allow a fine tuning of the spectrum flatness.

Fig. 9 provides the experimental results at 2700 km, after 9 round-trips in the loop. The optical signal-to-noise ratio (SNR) represented for even channels only and normalized to a 0.1 nm bandwidth is found to vary within [16.8 dB, 21.6 dB] and [16.8 dB, 21.6 dB] in C-band and L-band, respectively. The $Q$-factors of all 158 channels are also shown in Fig. 9, as derived from BER measurements. The worst $Q$ factor is 9.5 dB, which means that BERs are always better than $1.4 \times 10^{-3}$. With a concatenated FEC $[247, 239] + [255, 247]$, theory predicts that this value is 0.3 dB larger than the $Q$ factor yielding the BER threshold of $10^{-13}$ required for actual systems [1].

Based on the description of our latest laboratory experiment, showing the transmission of 6.3 Tbit/s data over a record 2700 km distance, we have illustrated some of issues dealt with in next generation WDM terrestrial networks. To transmit larger capacities within the available bandwidth of optical amplifiers, alternative modulation formats, such as PSBT, are advised. Specific optical amplifier configurations based on Raman amplifiers and erbium-doped fiber amplifiers can advantageously contain noise accumulation along the system and therefore extend the transmission distance.

## References


[1] E. Desurvire, D. Bayart, B. Desthieux, S. Bigo, Erbium-Doped Fiber Amplifiers: Device and System Developments, Wiley, New York, 2002, Chapter 7.
[2] G. Charlet et al., 6.4 Tb/s (159 × 42.7 Gb/s) capacity over 21 × 100 km using bandwidth-limited phase-shaped binary transmission, in: Proc. European Conf. Optical Communications, ECOC '02, Copenhagen, Denmark, September 8–12, PD4.1.
[3] B. Zhu et al., in: Proc. European Conf. Optical Communications, ECOC '02, Copenhagen, Denmark, September 8–12, PD4.2.
[4] A. Küng, A. Agarwal, S. Banerjee, D.F. Grosz, D.N. Maywar D, M. Movassaghi, T.H. Wood, in: Proc. European Conf. Optical Communications, ECOC '02, Copenhagen, Denmark, September 8–12, PD4.3.
[5] J.C. Rasmussen, A. Isomura, Y. Akiyama, Y. Qiao, G. Ishikawa, in: Proc. European Conf. Optical Communications, ECOC '02, Copenhagen, Denmark, September 8–12, PD4.4.
[6] C. Hullin, C. Gueritch, E. Grand, D. Lesterlin, S. Ruggeri, M. Adlerfligel, J.P. Blondel, V. Bouder, C. Trecasser, L. Curinckx, E. Brandon, O. Courtois, D. Filet, in: Proc. European Conf. Optical Communications, ECOC '02, Copenhagen, Denmark, September 8–12, 1.1.3.
[7] H. Bissessur, G. Charlet, E. Gohin, C. Simonneau, L. Pierre, W. Idler, in: Proc. European Conf. Optical Communications, ECOC '02, Copenhagen, Denmark, September 8–12, 8.1.2.
[8] G. Charlet et al., in: Proc. Topical Meeting on Optical Amplifiers and their Applications, OAA '02, Vancouver, Canada, July 14–17, PDP1.
[9] A.H. Gnauck et al., in: Proc. Optical Fiber Communications Conference, OFC '02, Anaheim, CA, March 17–22, FC2-1.
[10] Y. Frignac et al., in: Proc. Optical Fiber Communications Conference, OFC '02, Anaheim, CA, March 17–22, FC5-1.
[11] F. Liu et al., in: Proc. Optical Fiber Communications Conference, OFC '02, Anaheim, CA, March 17–22, FC7-1.
[12] B. Zhu et al., in: Proc. Optical Fiber Communications Conference, OFC '02, Anaheim, CA, March 17–22, FC8-1.
[13] S. Bigo et al., in: Proc. European Conf. Optical Communications, proc. European Conf. Optical Communications, ECOC '01, Amsterdam, The Netherlands, October 1–4, PD.M.1.1.
[14] H. Sotobayashi et al., in: Proc. European Conf. Optical Communications, ECOC '01, Amsterdam, The Netherlands, October 1–4, PD.M.1.3.
[15] B. Zhu et al., in: Proc. European Conf. Optical Communications, ECOC '01, Amsterdam, The Netherlands, October 1–4, PD.M.1.8.
[16] H. Bissessur et al., in: Proc. European Conf. Optical Communications, ECOC '01, Amsterdam, The Netherlands, October 1–4, PD.M.1.11.
[17] D.F. Grosz et al., in: Proc. European Conf. Optical Communications, ECOC '01, Amsterdam, The Netherlands, October 1–4, PD.B.1.3.
[18] E. Desurvire, Erbium-Doped Fiber Amplifiers, Principles and Applications, Wiley, New York, 2002, Chapter 7.
[19] D. Le Guen et al., in: Proc. Optical Fiber Communication Conf., OFC '99, San Diego, CA, February 21–26, PD-4.
[20] Y. Miyamoto et al., in: Proc. Optical Fiber Communication Conf., OFC '00, Baltimore, MD, March 3–10, PD-26.
[21] E.A. Golovchenko, A.N. Pilipetskii, N.S. Bergano, in: Proc. Optical Fiber Communication Conf., OFC '00, Baltimore, MD, March 3–10, Paper FC3.
[22] R. Ohhira, D. Ogasahara, T. Ono, in: Proc. Optical Fiber Communication Conf., OFC '01, Anaheim, CA, March 17–22, PD25.
[23] T. Tsuritani, A. Agata, I. Morita, K. Tanaka, and N. Edagawa, in: Proc. Optical Fiber Communication Conf., OFC '01, Anaheim, CA, March 17–22, Paper MM5.
[24] D. Penninckx, M. Chbat, L. Pierre, J.-P. Thiéry, IEEE Photon. Technol. Lett. 9 (1997) 259–261.
[25] H. Bissessur, L. Pierre, D. Penninckx, J.-P. Thiéry, J.-P. Hamaide, Electron. Lett. 37 (1) (2001) 45–46.